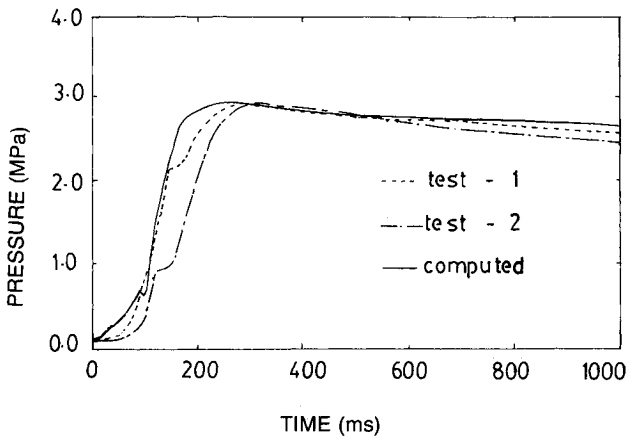

Fig. 2 Comparison of computed and measured pressure transients.

tion is computed by solving a one-dimensional heat conduction equation in the propellant. Critical ignition temperature criterion is applied to determine the point of ignition. Following ignition in the impingement and head-end regions, the mass flux generated from the propellant surface in these regions is calculated at every instant from the known burning rate law of the propellant. Based on the mass fractions of the igniter products and the generated gases at the motor propellant, the effective specific heat and temperature of the resultant mixture is calculated and is input at the left boundary for the downstream region.

Results

Computations have been performed using the method and the results compared with available test data. The test motor has a 8.6 m monolithic grain of AP-PBAN-A1 propellant system. The port is a six-pointed star configuration. The motor employs a canted-impingement-type pyrogen igniter with a cant angle of 45 deg. The impingement area amounts to 6% and the head-end area to 12% of the total initially exposed propellant burning surface area. The downstream region constitutes 87% of the grain length. A nozzle diaphragm, designed to burst at 0.6 MPa, is provided. Figure 2 compares the measured and computed pressure transients at the motor head end. The computations show a more rapid pressure drop upon nozzle diaphragm burst; this may be a consequence of assuming instantaneous diaphragm burst resulting in immediate availability of the full throat area for exhaust of combustion products, whereas the actural mechancial system may involve a small but finite time delay of a few milliseconds. The computed rate of pressurization is seen to be higher than the test values. This may be due to the limitation of the one-dimensional flow analysis, which implies instantaneous circumferential flame spread. The prediction procedure may be improved by a two-dimensional flow analysis.

References

[1]Peretz, A., "The starting Transient of Solid Propellant Rocket Motors with High Internal Gas Velocities," Aerospace and Mechanical Sciences Report No. 1100, Princeton University, Princeton, NJ, April 1973.

[2]Caveny, L. H. and Kuo, K. K., "Ignition Transients of Large Segmented Rocket Boosters," NASA CR-150162, April 1976.

[3]Caveny, L. H., "Extensions to Analysis of Ignition Transients of Segmented Rocket Motors," NASA CR-150632, Jan. 1978.

[4]Love, E. S., "Experimental and Theoretical Studies of Axisymmetric Free Jets," NASA TR-R-6, 1959.

[5]Martin, H., "Heat and Mass Transfer Between Impinging Gas, Jets and Solid Surfaces," *Advances in Heat Transfer*, Vol. 13, 1977.

Cesium Density Measurements with a Laser Diode in a Magnetohydrodynamic Generator

E. M. van Veldhuizen*
Eindhoven University of Technology, Eindhoven, the Netherlands

I. Introduction

THE development of magnetohydrodynamic (MHD) generators as a topping cycle in electrical power plants involves many aspects. Plasmaphysics, gasdynamics, and power electronics are the main topics. The work performed at the Eindhoven University of Technology is concentrated on the generator itself. Therefore, as many measurements as possible are carried out to obtain data of the plasma inside the channel.

In this Note, the cesium density measurement is described in detail. Other diagnostics are discussed elsewhere.[1] In the closed-cycle blowdown generator as used in our laboratory cesium is added to the argon gas to enhance conductivity. The amount of cesium can be adjusted as a weight fraction of the argon. The distribution of cesium in the generator, however, is unknown. By means of line absorption the density inside the generator can be measured, i.e., the ground state density of an atom is measured by the absorption of a resonance line. In the case of cesium there are two options: 894.4 and 852.1 nm, i.e., the near infrared. The lineshapes of these transitions are strongly influenced by collisions with the argon atoms. Accurate experimental data for the argon-cesium case are available.[2] The best signal-to-noise ratio is obtained from the experiment with a wavelength of 854.6 nm, i.e., 2.5 nm in the red wing of the 852.1-nm cesium line, as is pointed out in Ref. 1.

This wavelength is close to the wavelength of the GaAlAs laser diode. Since the wavelength of these lasers depends strongly on the temperature, some of them have a built-in Peltier element for temperature stabilization. This element can also be used to tune the wavelength within a region of several nanometers, thus obtaining the desired wavelength for the absorption measurement.

II. Laser Stabilization

The laser used here is a TXSK 3501 made by AEG-Telefunken with a nominal wavelength of 850 nm and a maximum output power of 10 mW at a current of 150 mA. Built in are a Peltier element, an NTC resistor, and a monitor diode. The laser is multimode. Its mode spacing is approximately 0.25 nm, and 10–20 modes are present depending on the output power. The wavelength is selected with a 1-m Jobin-Yvon monochromator, and the intensity is measured with a photomultiplier with a GaAs cathode (Hamamatsu R636). Using a slit width of 0.1 mm, this monochromator selects the wanted mode. A disadvantage could be that 90% of the output power of the laser is not used, but for this experiment the remaining 10% is satisfactory.

When the laser is cooled with the Peltier element the wavelength shifts toward the red. The wavelength of maximum power can thus be tuned from 838 to 862 nm, according to the

Received April 1, 1988; revision received Jan. 1, 1989. Copyright © American Institute of Aeronautics and Astronautics, Inc. All rights reserved.

*Member of the Scientific Staff, Electrical Energy Systems Division, Department of Electrical Engineering.

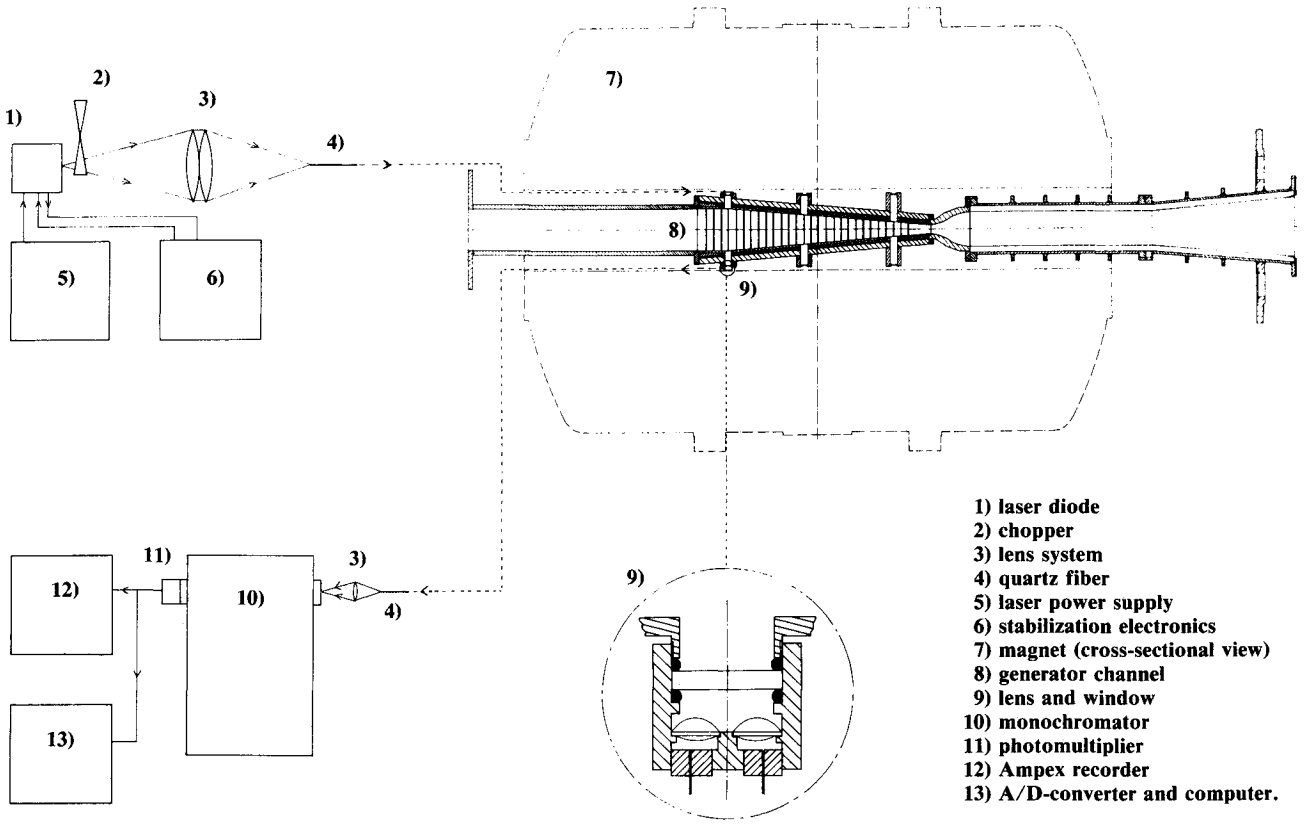

Fig. 1 Experimental setup.

specifications. A thermistor (NTC-resistor) is used for active stabilization of the temperature. This is done with a home-built proportional-integral controller. The time constant of the Peltier element with the thermistor is about 7 s, so the time constant of the circuit is set to 10 s to prevent oscillations. After tuning to the desired wavelength several readjustments are necessary at intervals of some minutes. Then the output is stable within 1% for several hours. Since the measuring time for one run is only 1 min, the stability is satisfactory. Readjustments must be made when the output power of the laser is changed, but once a good working point is known, it reproduces easily and almost exactly. The wavelength accuracy is 0.01 nm. This error is due to the monochromator.

III. Experimental Setup

For the transmission of optical signals from the badly accessible MHD channel quartz fibers with a core of 0.2 mm are used. No special treatment has been given to the front surface of the fiber so its insertion loss is about 5% for the air-glass transition. Because of the low specific loss (0.012 dB/m at 850 nm) a fiber of 30 m is used, with the advantage that the photomultiplier is easily shielded from the magnetic field. Compared with the previous setup with many mirrors, lenses, and beamsplitters the transmission of this system is increased by a factor of 100.

In Fig. 1 a schematic drawing of the setup is given. The output beam of the laser (1) is chopped (2) in order to distinguish the laser light from the light originating from the generator. Then the light is collected by a system of achromatic lenses (3) with an aperture of f/1, which focuses the light on the fiber (4). At the channel wall an aspherical lens (9) is mounted (f = 8 mm, $\phi = 12.5$ mm), which makes the beam parallel. Sapphire windows with a diameter of 25 mm are fixed gastight to the wall. The laser beam crosses the channel (8) and enters into another aspherical lens that focuses the light into the returning fiber. A lens couples the light of this fiber with the optimum aperture into the 1-m monochromator (10). The signal of the photomultiplier is directly recorded with a high-speed tape recorder (12) (Ampex FR 3000, DC-500 kHz) and an A/D (analog-to-digital) converter (13) with a sampling frequency of 4 Hz (filtered at 2 Hz). Behind each sapphire window there are three lenses with fibers. With the second the intensity of an He-Ne laser is monitored through an interference filter, giving an indication of the decay of the window transparency during the measurements. The third fiber is used for the measurement of radiation coming from the plasma.[3]

The measurements reported here have been carried out during measurement series 8 of the Eindhoven MHD Blow-Down Facility. More details about the experimental conditions can be found in Refs. 4 and 5.

IV. Results and Discussion

In Figs. 2 and 3 two pictures are given of signals recorded with the A/D-converter. Figure 2 is made with the laser diode. The cesium injection is started at $t = 18$ s and stopped at $t = 57$ s. The difference between the signals at the beginning and the end of the picture is an indication of cesium condensation on the saffire windows. At $t = 71$ s a valve is closed to prevent further condensation. Figure 3 is from a previous measurement where a xenon lamp is used. The cesium injection is started at $t = 28$ s. The increase of the signal between $t = 33$ and $t = 60$ s is because of the emission of the plasma during power extraction. During this run window transparency strongly decreased. In Fig. 2 nothing is seen from the background light of the generator, whereas in Fig. 3 the influence of the power extraction can be recognized in the signal between $t = 36$ and 62 s. This means that here the light originating from the generator is stronger than the light of the lamp. This is because in the experiment with the lamp a ¼-m monochromator had to be used with a slit of 0.6 mm in order to obtain enough signal from the lamp. This leads to the conclusion that the spectral power density of the laser is about two orders of magnitude higher than

Table 1 Cesium density measured in the MHD generator for several runs

Run	1[a]	2[b]	Run	1[a]	3[c]	Run	1[a]	3[c]
702	0.11	0.17	805	0.06	0.14	817	0.09	0.27
704	0.14	0.24	808	0.10	0.22	823	0.07	0.28
705	0.13	0.19	809	0.07	0.15	825	0.05	0.24

[a]Averaged value obtained from the injected mass. [b]Value obtained from the absorption measurement using the xenon lamp. [c]As b, but with the laser diode. All values are in percentages of the number density of argon.

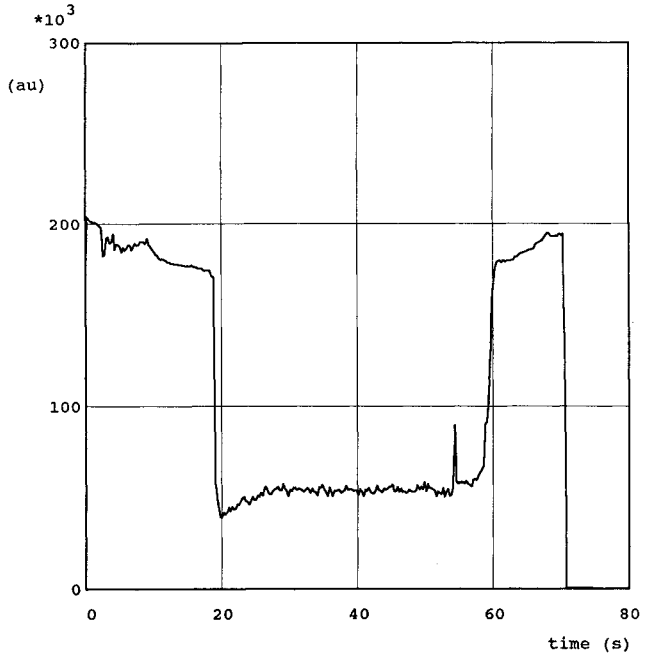

Fig. 2 Example of the absorption signal taken with the low-frequency A/D converter using the laser diode as source.

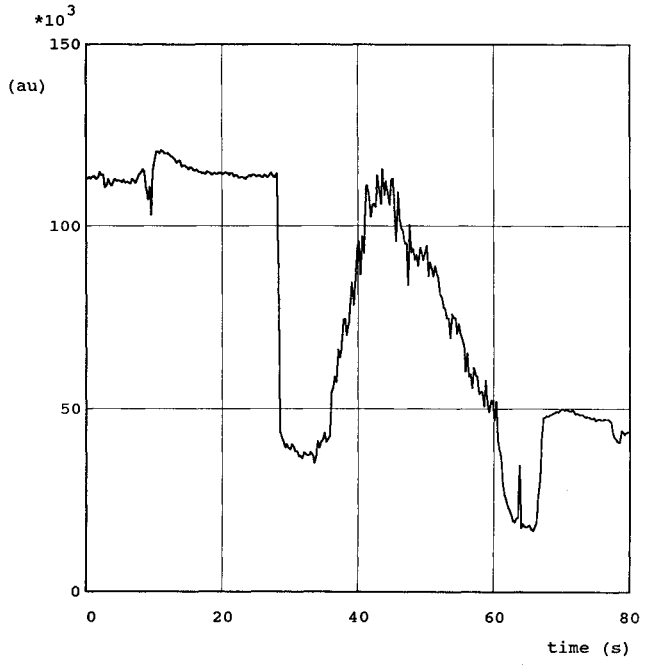

Fig. 3 Example of the absorption signal taken with the low-frequency A/D converter using the xenon lamp as source.

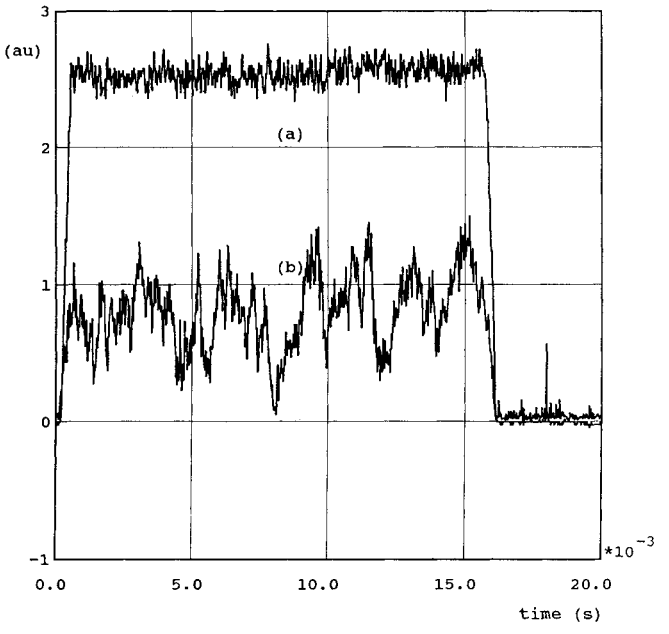

Fig. 4 Signal of the absorption measurement directly recorded with the Ampex using the diode laser as source. Trace (a) is taken before cesium is added. Trace (b) is with cesium and during power extraction. The electrical signal is filtered at 30 kHz.

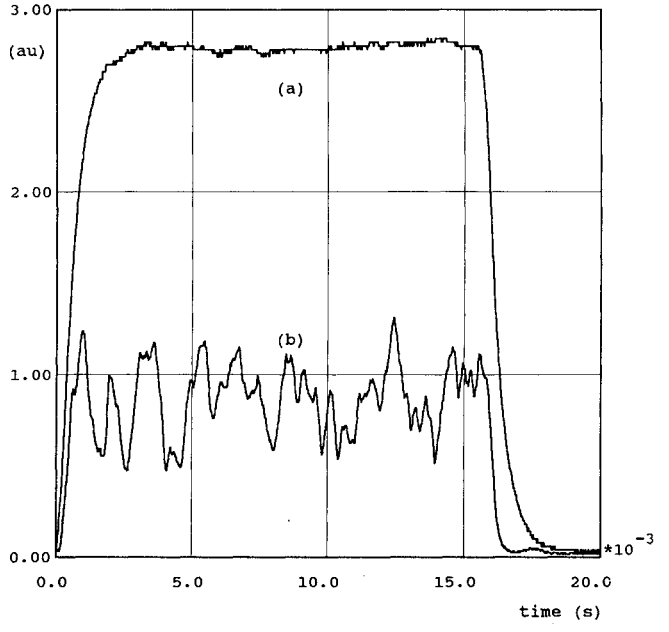

Fig. 5 As Fig. 4, but with a filter frequency of 1 kHz.

that of the lamp (in the region transmitted by the monochromator).

The average cesium density calculated from these pictures shows a discrepancy with the density calculated from the amount of cesium injected (see Table 1). In the latter case a uniform distribution is assumed, which is certainly not the case. For this calculation the width of the channel is taken from wall to wall. However, in the former case the line of sight between the two sapphire windows is much larger. Both effects lead to a higher value of the cesium density for the absorption measurement. This is confirmed by the results given in Table 1. The increasing discrepancy between columns 1 and 3 for the last three runs is explained by the decreasing window transparency, which leads to larger experimental uncertainties. During the last 15 runs of the measurement series this transparency decreased by a factor of more than 100 for a pair of windows.

Pictures made from the signals recorded directly on the Ampex show an unexpected behavior (see Figs. 4 and 5). There are large fluctuations in the absorption signal on a time scale of 1 ms. These fluctuations are present with and without power extraction. Fourier transforms of the signals show a more or less constant spectrum between 30 and 1000 Hz and a rapid decay beyond 1 kHz. Figures 4 and 5 show two signals: a) before cesium addition and b) during power extraction. From $t = 0$ to $t = 16$ ms the chopper is open; beyond $t = 16$ ms the chopper is closed, and no light from the generator is recorded. In Fig. 4 the signal is filtered at 30 kHz, in Fig. 5 at 1 kHz. The high-frequency noise in Fig. 4 originates from the tape recorder. The cesium density corresponding to the maximum and minimum of the absorbed signal varies by a factor of two.

V. Conclusion

Replacing a high-pressure xenon lamp as a light source for absorption measurements by a GaAlAs laser diode yields a substantial improvement. Temperature stabilization with the built-in Peltier element and thermistor is easily achieved. The single mode with the highest intensity is selected with a monochromator. The stability of the output power in this single mode is better than 1% for several hours. The spectral output power density is about 100 times higher than that of the xenon lamp. The spontaneous emission of the plasma is not detected when the diode laser is used as the source in a cesium density measurement in an MHD generator. This allows a determination of the cesium density during the power extraction, and the signal is strong enough to obtain a high time resolution. A demonstration of the power of this measurement is the observation of fluctuations of a factor of two in the cesium density, within a millisecond, in an MHD generator during power extraction.

Acknowledgments

This work was performed with financial support from the Netherlands Department of Economic Affairs and the Stichting voor de Technische Wetenschappen (STW). The author wishes to thank R. Damstra, A. P. C. Holten, and C. H. F. M. van de Weem for their valuable contributions to the experiments; also, the author wishes to acknowledge the helpful discussions with W. F. H. Merck, L. H. Th. Rietjens, and A. Veefkind.

References

[1]van Veldhuizen, E. M., and Flinsenberg, H. J., "Methods and Results of Diagnosis in a Closed-Cycle MHD Blowdown Generator," *Journal of Propulsion and Power,* Vol. 3, No. 6, Nov. 1987, pp. 542–551.

[2]Chen, C. L., and Phelps, A. V., "Absorption Coefficients for the Wings of the First Two Resonance Doublets of Cesium Broadened by Argon," *Physical Review,* Vol. A7(2), Feb. 1972, pp. 470–479.

[3]van Veldhuizen, E. M., and Holten, A.P.C., "An Overview of Diagnostic Results of the EUT Blow-Down Generator," *Proceedings of the 26th Symposium on Engineering Aspects of Magnetohydrodynamics,* Nashville, TN, 1988, pp. 9.3.1–9.3.8.

[4]Balemans, W.J.M., and Rietjens, L.H.T., "High Enthalpy Extraction Experiments with the Eindhoven Blow-Down Facility," *Proceedings of the 9th International Conference on MHD Electrical Power Generation,* Vol. 2, Tsukuba, Japan, 1986, pp. 230–240.

[5]Balemans, W.J.M., Massee, P., and Rietjens, L.H.T., "Construction and Operation of the Eindhoven MHD Blow-Down Facility," *Proceedings of the 26th Symposium on Engineering Aspects of Magnetohydrodynamics,* Nashville, TN, 1988, pp. 2.4.1–2.4.8.

Steady Flow Combustion Model for Solid-Fuel Ramjet Projectiles

Michael J. Nusca*
U.S. Army Ballistic Research Laboratory, Aberdeen Proving Ground, Maryland

Nomenclature

c_p	= specific heat at constant pressure
h	= heat of formation
h_{vap}	= heat of vaporization per unit mass
$\tilde{h}$	= total enthalpy
k	= turbulence kinetic energy
M	= molecular weight
m	= mass fraction
$\dot{m}$	= mass flow rate
n	= stoichiometric air/fuel mass ratio
$\hat{n}$	= normal direction
p	= static pressure
q	= heat flux
$\Re$	= universal gas constant
R	= reaction rate per unit volume
r	= radial direction
$\dot{r}$	= solid fuel regression rate
Sc	= Schmidt number
T	= temperature
u	= velocity component in the axial direction
V	= magnitude of the local velocity vector
v	= velocity component in the azimuthal direction
w	= velocity component in the radial direction
z	= axial direction
Γ	= diffusion coefficient, μ_{eff}/Sc
ϵ	= turbulence dissipation rate
κ	= thermal conductivity
μ	= viscosity
ρ	= density
ϕ	= general flow variable
ψ	= stream function
ω	= vorticity

Subscripts

eff	= effective
fo	= fuel-oxidizer
fp	= fuel-products
fu	= fuel

Presented as Paper 89-2797 at the AIAA 25th Joint Propulsion Conference, Monterey, CA, July 10–12, 1989; received April 20, 1989; revision received Aug. 2, 1989. This paper is declared a work of the U.S. Government and is not subject to copyright protection in the United States.

*Aerospace Engineer, Launch and Flight Divisoin. Member AIAA.